A Generalized Gene-Regulatory Network Model of Stem Cell Differentiation for Predicting Lineage Specifiers

Satoshi Okawa,[1] Sarah Nicklas,[2] Sascha Zickenrott,[1] Jens C. Schwamborn,[2] and Antonio del Sol[1,*]

[1]Computational Biology Group
[2]Developmental and Cellular Biology Group
Luxembourg Centre for Systems Biomedicine, University of Luxembourg, 7 Avenue des Hauts Fourneaux, 4362 Esch-sur-Alzette, Luxembourg
*Correspondence: antonio.delsol@uni.lu
http://dx.doi.org/10.1016/j.stemcr.2016.07.014

SUMMARY

Identification of cell-fate determinants for directing stem cell differentiation remains a challenge. Moreover, little is known about how cell-fate determinants are regulated in functionally important subnetworks in large gene-regulatory networks (i.e., GRN motifs). Here we propose a model of stem cell differentiation in which cell-fate determinants work synergistically to determine different cellular identities, and reside in a class of GRN motifs known as feedback loops. Based on this model, we develop a computational method that can systematically predict cell-fate determinants and their GRN motifs. The method was able to recapitulate experimentally validated cell-fate determinants, and validation of two predicted cell-fate determinants confirmed that overexpression of ESR1 and RUNX2 in mouse neural stem cells induces neuronal and astrocyte differentiation, respectively. Thus, the presented GRN-based model of stem cell differentiation and computational method can guide differentiation experiments in stem cell research and regenerative medicine.

INTRODUCTION

Cellular phenotypes are characterized by stable gene-expression states determined by underlying gene-regulatory networks (GRNs), particularly by subnetworks that appear frequently and are functionally important (i.e., GRN motifs). A classical GRN motif, the toggle switch, constitutes a molecular mechanism that determines cell-fate decisions, and provides stability to transcriptional programs of binary cell-fate choices. Overexpression of each transcription factor (TF) corresponds to one of the two mutually exclusive cell fates, whereas a "balanced" expression of both TFs maintains the stem/progenitor state (Huang et al., 2007; Jacob and Monod, 1961; Roeder and Glauche, 2006). The toggle switch has been experimentally shown to play an important role in binary cell-fate control of stem/progenitor cells (Graf, 2002; Lin et al., 2008; Ralston and Rossant, 2005). A well-known example is the one consisting of an erythroid determinant *Gata1* (Pevny et al., 1991) and a myeloid determinant *Spi1* (Voso et al., 1994) in the hematopoietic stem cell (HSC) system.

Interestingly, a different GRN motif has been more recently proposed for explaining mesendodermal and ectodermal specification of mouse embryonic stem cells (mESCs) (Shu et al., 2013). In this motif, the balanced expression (i.e., similar expression levels) of a mesendodermal and an ectodermal cell-fate determinant, POU5F1 (Niwa et al., 2000; Zeineddine et al., 2006) and SOX2 (Kopp et al., 2008), respectively, maintains the pluripotent state, whereas significant up- or downregulation of either of these genes induces differentiation into the respective lineage. Moreover, replacing POU5F1 with other mesendo-

dermal determinants was able to induce reprogramming of fibroblasts to pluripotency in both mouse and human (Montserrat et al., 2013; Shu et al., 2013). These observations suggest that stem/progenitor cell states in general seem to be maintained by a balance between differentiation forces exerted by groups of opposing cell-fate determinants, and that the underlying GRN motifs do not necessarily comprise toggle switches. Indeed, a toggle switch belongs to a more general class of network motifs, known as feedback loops (Thomas, 1978; Siebert, 2009; Zañudo and Albert, 2013).

Taking these facts together, here we propose a computational model that generalizes binary-fate stem cell differentiation events (Figure 1), according to which stem/progenitor cells correspond to stable gene-expression states maintained by the balanced expression of cell-fate determinants residing in clusters of interconnected feedback loops (strongly connected components). Furthermore, these strongly connected components consist of differentially expressed TFs between two daughter cell types from the stem/progenitor cells, and stabilize the two stable gene-expression states corresponding to these two daughter cell types. Upregulated TFs in one of the daughter cells cooperate among themselves and compete with those upregulated in the other daughter cell.

Based on this model, we further propose a Boolean network-based computational method that can systematically predict cell-fate determinants and the GRN motifs to which these genes belong. This method is general, since it can be applied to any stem cell differentiation system for which gene-expression data of the stem/progenitor and the two daughter cells are available. We selected five
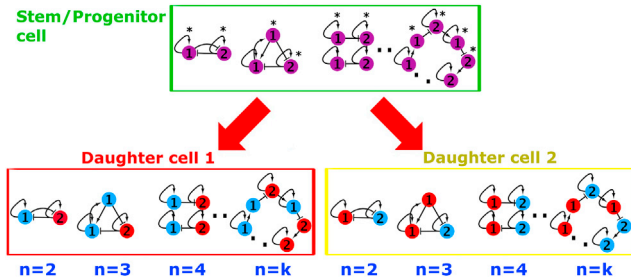
Figure 1. Proposed Model of Binary-Fate Stem Cell Differentiation Governed by GRN Motifs

In this model two different daughter cell types (daughter 1 and daughter 2) from a common stem/progenitor cell correspond to two stable steady states, which are stabilized by strongly connected components of any number of genes consisting of differentially expressed TFs between two daughter cells. The same strongly connected components are used for maintaining the stem/progenitor state, in which pair(s) of TFs exhibit a more balanced expression pattern in comparison with that in two daughter cells (indicated by asterisks). TFs that do not show this balanced expression pattern are still necessary for stabilizing the expression balance of TFs marked with asterisks. The classical toggle switch that consists of two TFs (n = 2) is the simplest case of this model. Red nodes are TFs upregulated in daughter 1. Blue nodes are TFs upregulated in daughter 2. Purple nodes indicate TF expression in the stem/progenitor cell. Pointed arrows indicate activation and blunted arrows indicate inhibition. Note that motifs shown in this figure are examples of each n. Motifs with different topologies (not shown) are possible.

stem cell systems to assess the validity of the method: mESCs, mHSCs, mouse neural stem cells (mNSCs), mouse mesenchymal stem cells (mMSCs), and hESCs differentiating into MESP1$^+$ or MESP1$^-$ (pre-)cardiac progenitor cells (hCPCs) (den Hartogh et al., 2015). Our predictions were able to recapitulate experimentally validated cell-fate determinants in these systems. In particular, the method predicted known cell-fate determinants in the hCPC system, where the differentiation is incomplete and phenotypic differences between the two daughter cells are relatively small. Finally, we experimentally validated predicted cell-fate determinants in the mNSC system, which confirmed that ESR1 and RUNX2 induce neuronal and astrocyte differentiation, respectively.

Thus, this study presents a general GRN-based computational model that can identify GRN motifs crucial for both maintenance and differentiation of stem/progenitor cells. From a systems biology point of view, identification of functionally important subnetworks is important for extracting biologically meaningful information from a large GRN. Finally, the method solely requires transcriptome data and literature knowledge of TF interactions, while not requiring prior knowledge of potential candidate genes; neither are pathways or gene ontology necessary.

Therefore, our approach offers practical guidance to experiments in stem cell biology and regenerative medicine.

RESULTS

The Method Recapitulates Known Toggle Switches

The overview of our computational method is shown in Figures 2 and S4. In brief, a Boolean GRN among differentially expressed TFs between two daughter cell types is reconstructed using database knowledge and our network-pruning algorithm. In parallel, pairs of TFs whose expression patterns are significantly disrupted upon differentiation in comparison with the stem/progenitor cell are identified. In each of these significant TF pairs, if the two TFs are directly connected to each other in their respective most frequent strongly connected component, they are considered candidate cell-fate determinants (see Experimental Procedures for details). Application of this method was able to recapitulate the well-characterized toggle switches for the *Gata1-Spi1* pair (Graf, 2002) and the *Runx2-Pparg* pair (Lin et al., 2008) in the mHSC and mMSC systems, respectively (Figures 3B and 3E). Note that the statistical metric we devised in this study, the normalized ratio difference (NRD), was intended to identify pairs of TFs whose expression ratios showed a significant change in daughter cells in comparison with the stem/progenitor cells. We suggest that the NRD is biologically more relevant than the absolute ratio within each cell type, since the basal/effective level of expression differs among different TFs. Indeed, the expression values of the two TFs in well-known pairs, such as *Gata1-Spi1* and *Runx2-Pparg*, were very different in the progenitor cells (Table 1). The TF pairs with significant NRD (significant NRD TF pairs) in each system are listed in Table S1.

The Predicted GRN Motif Explains Previous Experimental Evidence in mESCs

It has been shown that induced pluripotent stem cells (iPSCs) could be derived by expressing KLF4 and POU5F1 in SOX2-expressing mouse neural progenitor cells (Blelloch et al., 2006), or in mouse embryonic fibroblasts in combination with small compounds that can substitute SOX2 (Shi et al., 2008). These previous observations suggest that KLF4 acts similarly to POU5F1 and antagonistically to SOX2. In addition, *PAX6* is a known ectoderm determinant in human (Zhang et al., 2010). Therefore, the mESC GRN motif predicted for the *Pou5f1-Sox2* pair in this study (consisting of *Pou5f1*, *Sox2*, *Klf4*, and *Pax6*) (Figure 3A and Table 1) can mechanistically explain these previous experimental observations. In addition, this motif resembles the one previously proposed (Shu et al., 2013), which consisted of two nodes representing *Pou5f1* and
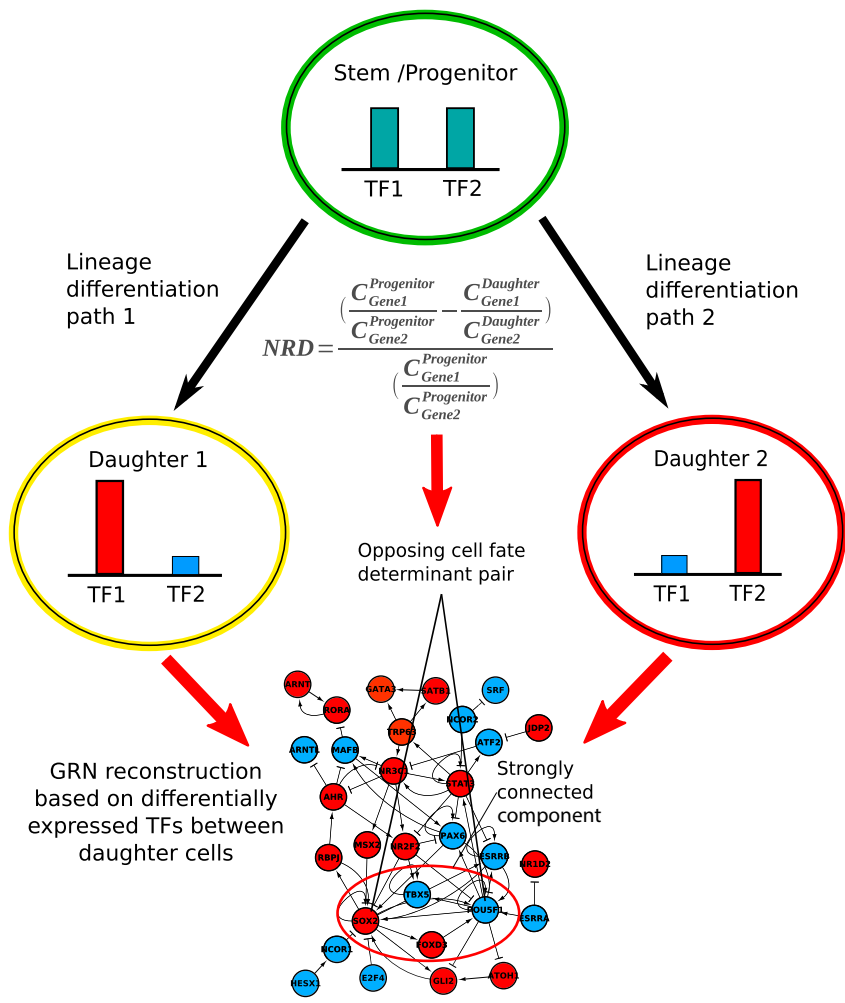
$$NRD = \frac{\left(\dfrac{C_{Gene1}^{Progenitor}}{C_{Gene2}^{Progenitor}} - \dfrac{C_{Gene1}^{Daughter}}{C_{Gene2}^{Daughter}} \right)}{\left(\dfrac{C_{Gene1}^{Progenitor}}{C_{Gene2}^{Progenitor}} \right)}$$

Figure 2. Schematic View of Proposed Method

Differentially expressed genes are computed between two daughter cells and Boolean GRNs are reconstructed from differentially expressed TFs by first retrieving literature-based interactions and then pruning this network by removing interactions incompatible with Booleanized gene-expression data of two daughter cells. In parallel, statistically significant NRD TF pairs are computed. Finally, for each significant NRD TF pair, the most frequent strongly connected component is identified among the best GRN solutions. If two paired TFs are directly connected to each other in that strongly connected component, they are considered predicted opposing cell-fate determinants together with their GRN motif.

Sox2 and two hyper-nodes (i.e., collections of unknown genes) representing the ectoderm and mesoderm, further supporting our proposed general differentiation model. Importantly, our method does not use hyper-nodes, so it can explicitly describe key interactions among cell-fate determinants that collectively maintain different cellular identities.

The Method Predicted Known Lineage Specifiers Even when Differentiation Is Incomplete

The method was also applied to the dataset of CPC differentiation, in which hESCs were differentiated into MESP1⁺ and MESP1⁻ (pre-)CPCs (den Hartogh et al., 2015), where only the former was able to differentiate further into cardiomyocytes. Our predictions of cell-fate determinants for the MESP1⁺ lineage included *GATA4*, a well-known inducer of cardiac differentiation (Kuo et al., 1997) (Figure 3F), and *MYC*, which has recently been shown to play a critical role in long-term expansion of CPCs (Birket et al., 2015) (Table 1). Hence, our method was able to predict important

cardiac cell-fate determinants even when the differentiation is not terminal and the two daughter cell types are close to each other. This aspect of the method can be useful when differentiation into a not well-defined particular subtype of a cell lineage is desired.

Deterministic Continuous Simulation Reproduces Expected Differentiation Dynamics upon Perturbations

An advantage of our method is that it is solely based on a simple Boolean network model for its predictions. However, because the Boolean model might oversimplify the quantitative nature of real biology, such as the inability to represent an intermediate steady state for stem/progenitor cells, we next investigated whether predicted GRN motifs could capture expected cell-fate decisions in a more realistic continuous model (see Supplemental Experimental Procedures for details). The mHSC system was used for this purpose, as it is the most well studied both experimentally and theoretically. The result indicates that our
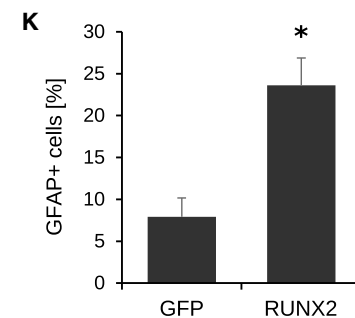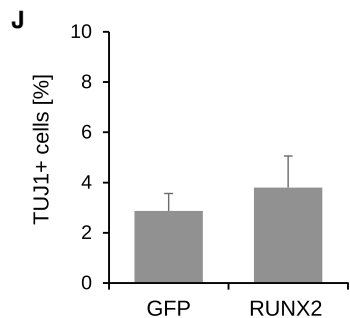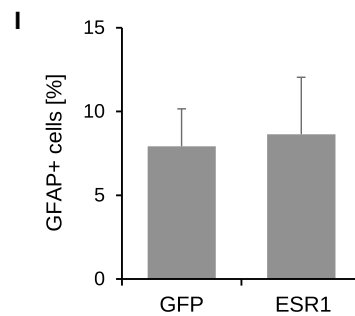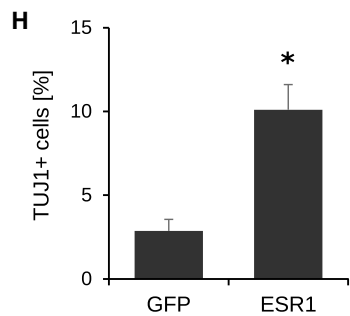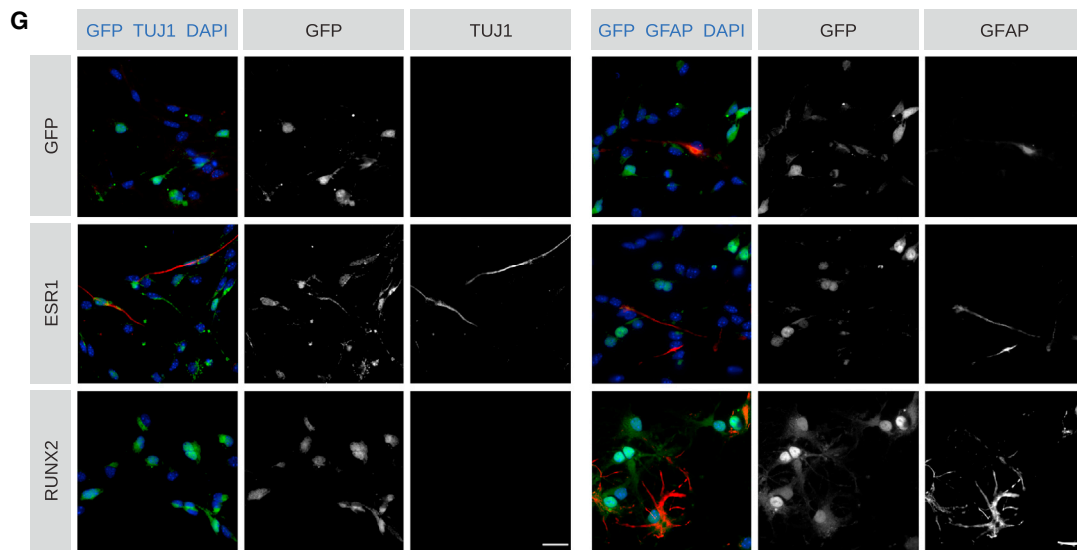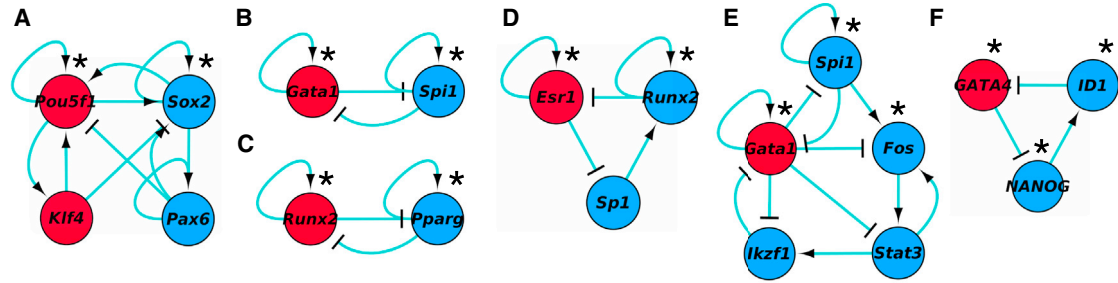
Figure 3. Predicted Opposing Cell-Fate Determinant Pairs, Their GRN Motifs, and Their Experimental Validation in mNSCs

(A–F) Red nodes are TFs upregulated in daughter 1 (mesoderm, erythroid, neuron, osteoblast, and MESP1^{+} CPC). Blue nodes are TFs up-regulated in daughter 2 (ectoderm, myeloid, astrocyte, adipocyte and MESP1^{−} CPC). Pointed arrows indicate activation, blunted arrows

(legend continued on next page)

Table 1. Predicted Opposing Cell-Fate Determinant Pairs, Their Minimum Out-Degree Interface, Number of TFs in Their GRN Motifs, Microarray Expression Values, and Figure Locations

Best Candidate Opposing Cell-Fate Determinant Pair	Minimum Out-Degree Interface	No. of TFs in Strongly Connected Component	Log$_2$(Expression) Value in Progenitor	Log$_2$(Expression) Value in Daughter 1	Log$_2$(Expression) Value in Daughter 2	Figure
1. mESC						
Pou5f1-Sox2	8	4	10.63__11.05	4.26__3.13	2.58__7.85	3A
Sox17-Sox2	20	8	9.75__11.05	0.74__7.85	4.59__3.13	S1A
2. mHSC						
Gata1-Fos	16	5	12.57__7.12	14.87__6.24	12.21__10.75	3E
Gata1-Cebpa	16	4	12.57__10.44	14.87__10.03	12.21__12.37	S1B
Gata1-Spi1	12	2	12.57__8.26	14.87__6.77	12.21__10.04	3B
Gata1-Gata2	10	5	12.57__14.79	14.87__15.69	12.21__16.88	S1C
Cux1-Irf1	4	8	10.40__13.38	10.56__11.95	9.51__14.64	S1D
3. mNSC						
Esr1-Runx2	6	3	4.03__3.74	7.24__5.20	4.97__7.30	3D
Esr1-Stat5a	5	5	4.03__4.74	7.24__5.37	4.97__6.70	S1E
Mef2c-Hey1	1	6	6.82__5.67	13.14__9.52	8.67__11.05	S1F
4. mMSC						
Runx2-Pparg	4	2	5.27__7.11	10.13__4.25	5.25__11.96	3C
5. hCPC						
MYC-PBX1	6	4	10.11__9.03	10.24__7.48	9.48__9.02	S1G
MYC-NANOG	6	4	10.11__8.93	10.24__7.07	9.48__9.29	S1G
GATA4-NANOG	3	2	6.70__8.93	8.25__7.07	7.45__9.29	3F
GATA4-ID1	2	3	6.70__12.48	8.25__10.06	7.45__12.28	3F

Columns 4–6 indicate normalized log$_2$ microarray expression values. "Progenitor" indicates hESCs, mHSCs, mNSCs, mMSCs, and hESCs, "daughter 1" indicates ectoderms, erythroids, neurons, osteoblasts, and MESP1$^+$ CPCs, and "daughter 2" indicates mesoderms, myeloids, astrocytes, adipocytes and MESP1$^-$ CPCs, respectively. Left TF and right TF in each pair are predicted cell-fate determinants for daughter 1 and daughter 2, respectively, when overexpressed. See Experimental Procedures for the definition of minimum out-degree interface.

continuous simulation recapitulated the known dynamics of the *Gata1-Spi1* toggle switch (Figure 3B), in which the progenitor state remained stable over time but reached the erythroid state when either GATA1 was upregulated or SPI1 was downregulated (Huang et al., 2007) (Figure S2). On the other hand, the opposite myeloid differentiation dynamics was also reproduced (Figure S2). In addition, the more complex five-gene motif for the *Gata1-Fos* pair, which includes the *Gata1-Spi1* toggle switch (Figure 3E), also exhibited the tristability corresponding to the three cell types, and reached the expected erythroid or myeloid state upon appropriate perturbation of any gene in the

indicate inhibition. Asterisks indicate TFs that showed a significant NRD. GRN motifs of (A) *Pou5f1-Sox2* pair in mESCs, (B) *Gata1-Spi1* pair in mHSCs, (C) *Runx2-Pparg* pair in mMSCs, (D) *Esr1-Runx2* pair in mNSCs, (E) *Gata1-Fos* pairs in mHSCs, and (F) *GATA4-NANOG* and *GATA4-NANOG* pairs in hCPCs.
(G) Lineage marker (TUJ1 and glial fibrillary acidic protein [GFAP]) immunostaining of cells cultivated under maintenance conditions for 5 days after transduction with lentiviruses encoding GFP (negative control), ESR1, or RUNX2. Scale bar, 20 μm.
(H–K) Diagrams showing the percentage of TUJ1-positive (H, J) and GFAP-positive (I, K) cells transduced with lentiviruses encoding GFP, ESR1, or RUNX2 (mean ± SEM; n ≥ 420 cells, N = 3 independent mNSC cultures; *p < 0.05, t test).

motif (Figure S3). Hence, this continuous simulation study demonstrates that, although our Boolean network-based method does not consider the intermediate stem/progenitor attractor state, the predicted GRN motif exhibited the appropriate differentiation dynamics upon perturbation of its genes.

ESR1 Induces Neuronal Differentiation and RUNX2 Induces Astrocyte Differentiation

To our knowledge, no well-defined cell-fate determinant pair and their GRN motif are known for the mNSC system. Our method predicted the *Esr1-Runx2* pair as the top candidate (Table 1), which stabilizes the three cell types via a three-gene GRN motif (Figure 3D). To validate this prediction, we performed the lentiviral transduction experiment under mNSC maintenance conditions (Conti et al., 2005). We used these conditions rather than differentiation-inducing conditions, since the latter will have a mixture of influences (i.e., both transduced TF and differentiation signals coming from the media) and it is difficult to draw clear conclusions under these conditions. The result confirmed a significant increase in the amount of neuron-specific class III β-tubulin (TUJ1)-positive cells upon overexpression of ESR1 in mNSCs (from 2.9% to 10%) (Figures 3G and 3H). Importantly, it did not induce astrocyte differentiation (Figures 3G and 3I). Conversely, overexpression of RUNX2 strongly induced astrocyte differentiation (from 8% to 24%) (Figures 3G and 3K), but this effect was restricted to the astrocyte lineage only (no increase in TUJ1-positive cells) (Figures 3G and 3J). These data demonstrate that the predicted function of TF pairs to induce lineage specifications can be validated experimentally, indicating the applicability of the method described here to stem cell differentiation experiments in general. Although our method has been shown to predict cell-fate determinants for different cell lineages, including neurons and astrocytes, it can also be applied for more specific cell subtypes, such as dopaminergic neurons or subventricular zone astrocytes. In these cases additional cell type specific markers would be required.

DISCUSSION

The interest in directed cell-fate determination in stem cell biology and regenerative medicine has been increasing over the years. However, due to the complexity of GRNs, identification of cell-fate determinants and their functionally important subnetworks (GRN motifs) that determine stem cell maintenance and differentiation remains a challenge. Indeed, there have been a few attempts to model cellular conversions by means of network biology

(Crespo and del Sol, 2013; Cahan et al., 2014; Zañudo and Albert, 2015; Rackham et al., 2016; Jo et al., 2016) using bulk transcriptome data. These previous studies deal with transitions between two well-defined cell types, such as reprogramming. As a complementary approach to these studies, the present study provides a generalized network model of stem/progenitor differentiation, providing insights into how pluri-/multipotent stem/progenitor cells capable of differentiating into multiple distinct lineages are maintained by the balanced gene expression of cell-fate determinants. In addition, the applicability of the aforementioned previous methods appears to be limited to cell types, for which not only transcriptome data but also other types of data, such as gene ontology and curated GRNs, are already available. The computational method presented in this study requires only bulk transcriptome data and literature knowledge of TF interactions.

Experimental validation of predicted cell-fate determinants confirmed that overexpression of ESR1 and RUNX2 in mNSCs induces neuronal and astrocyte differentiation, respectively. Indeed, it has been previously shown that overexpression of ESR1 was able to induce differentiation in neuroblastoma cells (Loven et al., 2010; Ma et al., 1993). In addition, embryonic rat NSCs have been shown to undergo neuronal differentiation in response to an ESR1 ligand, estradiol (Brannvall et al., 2002). However, until the present study evidence that overexpression of ESR1 is able to induce differentiation of mNSCs into neurons has been lacking. Furthermore, RUNX2 is well known for inducing differentiation of MSCs into osteoblasts (Banerjee et al., 1997; Ducy et al., 1997; Komori et al., 1997; Otto et al., 1997) but it has not been previously shown to induce astrocyte differentiation, which demonstrates how a same gene can have different lineage specification roles depending on the biological context characterized by GRN motifs. Interestingly, the induction of neuronal differentiation by ESR1 is not as strong as the induction of astrocytes by RUNX2. Most probably this is because the utilized mNSC system mimics the developmental stage of late radial glia cells, which are more primed toward the astrocyte fate (Conti and Cattaneo, 2010; Conti et al., 2005); consequently, their induction into this fate is easier than neuronal induction.

In sum, here we have proposed a generalized GRN-based computational model of stem cell differentiation and a computational method that systematically predicts cell-fate determinants and their GRN motifs. The generality and simplicity of this method makes it easy to apply to new cellular differentiation events, and therefore can assist in guiding experiments in stem cell biology and regenerative medicine.

EXPERIMENTAL PROCEDURES

Detection of TF Pairs Whose Expression Ratio Is Significantly Changed upon Differentiation

The test statistic NRD, determining whether a pair of genes is equally expressed in the parental cell in comparison with the daughter, cell is defined by

$$NRD = \frac{\left(\dfrac{C_{gene1}^{Progenitor}}{C_{gene2}^{Progenitor}} - \dfrac{C_{gene1}^{Daughter}}{C_{gene2}^{Daughter}}\right)}{\left(\dfrac{C_{gene1}^{Progenitor}}{C_{gene2}^{Progenitor}}\right)},$$

where $C_{gene1}^{Progenitor}$, $C_{gene2}^{Progenitor}$, $C_{gene1}^{Daughter}$, and $C_{gene2}^{Daughter}$ are the expression values of gene 1 and gene 2 in the progenitor cell and a daughter cell, respectively. This value was calculated for all pairs of TFs annotated in AnimalTFDB (http://www.bioguo.org/AnimalTFDB/download/gene_list_of_Mus_musculus.txt). Since the distribution of NRDs was not Gaussian, they were then normalized by median absolute deviation (MAD) normalization defined by

$$\widehat{X}_j = \frac{X_j - median}{MAD},$$

where X_j is the NRD of gene pair j and $\widehat{X}_j$ is the normalized NRD, and the median and MAD are computed based on all NRDs. This normalized NRD was computed for each microarray replicate, and the moderated t significance test of this statistic was performed using the limma R package. The Benjamini-Hochberg multiple test correction was then applied with a false discovery rate cutoff of 0.05. This procedure was applied to each of the two cell lineages (two daughter cell types) separately, and TF pairs that had a significant NRD in both lineages in the opposite ratio directions were taken as the final set. We call these gene pairs "significant NRD TF pairs." Note that this p-value cutoff was set arbitrarily; however, the stringency can be adjusted by this p-value cutoff as well as that for the initial differential gene-expression test.

Prediction of Cell-Fate Determinant Pairs and Their GRN Motifs

The flowchart of this part of the method is shown in Figure S4. Our model of stem cell differentiation states that stem/progenitor cells correspond to stable states maintained by the balanced expression of cell-fate determinants residing in clusters of interconnected feedback loops (strongly connected components), Therefore, our aim here is to identify strongly connected components that contain significant NRD TF pairs and stabilize the Boolean stable steady states of the two daughter cell types. However, if one is interested in how these GRN motifs are connected to other genes, the entire GRN can be looked up.

In each of the best GRN solutions the largest strongly connected component was first identified using the Graph::Directed Perl module (http://search.cpan.org/dist/Graph/lib/Graph.pod). Each strongly connected component was then decomposed into smaller strongly connected components by first finding the first 300 shortest path-elementary circuits from each node using the graphkshortestpaths.m program (http://www.mathworks.com/matlabcentral/fileexchange/35397-k-shortest-paths-in-a-graph-represented-by-a-sparse-matrix–yen-s-algorithm-/content/graphkshortestpaths.m). Here we employed shortest paths, since we later consider directly connected genes as candidate cell-fate determinants and paths longer than shortest paths are not necessary for this step. For each of these decomposed strongly connected components, the attractor states were computed from the Booleanized microarray expression data of the two daughter cell types. If these two attractors were mutually exclusive and 100% identical to the attractors of the original GRN and to their starting microarray data, the motif was kept for subsequent analyses. We discarded strongly connected components whose attractors are either all 0 or 1, since our target motifs need to contain at least one upregulated TF for both attractors as potential candidate lineage specifiers. For each significant NRD TF pair, the most frequent strongly connected component was searched among the best GRN solutions and if the two TFs in the pair were directly connected to each other in that strongly connected component, the pair was considered the final candidate opposing cell-fate determinant pair together with its GRN motif. Note that these criteria were stringently set in the present study to demonstrate the proof of concept of the method. However, they can be easily relaxed and a longer list of candidate pairs and motifs can be assessed. In each stem cell system, candidate opposing cell-fate determinant pairs were ranked by their minimum out-degree interface (i.e., the smaller number of genes regulated by one of the two genes within the pair), since a pair with a higher number of out-degree interface is more likely to have a higher regulatory influence on the GRN.

SUPPLEMENTAL INFORMATION

Supplemental Information includes Supplemental Experimental Procedures and four figures and can be found with this article online at http://dx.doi.org/10.1016/j.stemcr.2016.07.014.

REFERENCES

Banerjee, C., McCabe, L.R., Choi, J.Y., Hiebert, S.W., Stein, J.L., Stein, G.S., and Lian, J.B. (1997). Runt homology domain proteins in osteoblast differentiation: AML3/CBFA1 is a major component of a bone-specific complex. J. Cell Biochem. *66*, 1–8.

Birket, M.J., Ribeiro, M.C., Verkerk, A.O., Ward, D., Leitoguinho, A.R., den Hartogh, S.C., Orlova, V.V., Devalla, H.D., Schwach, V., Bellin, M., et al. (2015). Expansion and patterning of cardiovascular

progenitors derived from human pluripotent stem cells. Nat. Biotechnol. *33*, 970–979.

Blelloch, R., Wang, Z., Meissner, A., Pollard, S., Smith, A., and Jaenisch, R. (2006). Reprogramming efficiency following somatic cell nuclear transfer is influenced by the differentiation and methylation state of the donor nucleus. Stem Cells *24*, 2007–2013.

Brannvall, K., Korhonen, L., and Lindholm, D. (2002). Estrogen-receptor-dependent regulation of neural stem cell proliferation and differentiation. Mol. Cell Neurosci. *21*, 512–520.

Cahan, P., Li, H., Morris, S.A., Lummertz da Rocha, E., Daley, G.Q., and Collins, J.J. (2014). CellNet: network biology applied to stem cell engineering. Cell *158*, 903–915.

Conti, L., and Cattaneo, E. (2010). Neural stem cell systems: physiological players or in vitro entities? Nat. Rev. Neurosci. *11*, 176–187.

Conti, L., Pollard, S.M., Gorba, T., Reitano, E., Toselli, M., Biella, G., Sun, Y., Sanzone, S., Ying, Q.L., Cattaneo, E., et al. (2005). Niche-independent symmetrical self-renewal of a mammalian tissue stem cell. PLoS Biol. *3*, e283.

Crespo, I., and del Sol, A. (2013). A general strategy for cellular reprogramming: the importance of transcription factor cross-repression. Stem Cells *31*, 2127–2135.

den Hartogh, S.C., Schreurs, C., Monshouwer-Kloots, J.J., Davis, R.P., Elliott, D.A., Mummery, C.L., and Passier, R. (2015). Dual reporter MESP1 mCherry/w-NKX2-5 eGFP/w hESCs enable studying early human cardiac differentiation. Stem Cells *33*, 56–67.

Ducy, P., Zhang, R., Geoffroy, V., Ridall, A.L., and Karsenty, G. (1997). Osf2/Cbfa1: a transcriptional activator of osteoblast differentiation. Cell *89*, 747–754.

Graf, T. (2002). Differentiation plasticity of hematopoietic cells. Blood *99*, 3089–3101.

Huang, S., Guo, Y.P., May, G., and Enver, T. (2007). Bifurcation dynamics in lineage-commitment in bipotent progenitor cells. Dev. Biol. *305*, 695–713.

Jacob, F., and Monod, J. (1961). Genetic regulatory mechanisms in the synthesis of proteins. J. Mol. Biol. *3*, 318–356.

Jo, J., Hwang, S., Kim, H.J., Hong, S., Lee, J.E., Lee, S.G., Baek, A., Han, H., Lee, J.I., Lee, I., et al. (2016). An integrated systems biology approach identifies positive cofactor 4 as a factor that increases reprogramming efficiency. Nucleic Acids Res. *18*, 44.

Komori, T., Yagi, H., Nomura, S., Yamaguchi, A., Sasaki, K., Deguchi, K., Shimizu, Y., Bronson, R.T., Gao, Y.H., Inada, M., et al. (1997). Targeted disruption of Cbfa1 results in a complete lack of bone formation owing to maturational arrest of osteoblasts. Cell *89*, 755–764.

Kopp, J.L., Ormsbee, B.D., Desler, M., and Rizzino, A. (2008). Small increases in the level of Sox2 trigger the differentiation of mouse embryonic stem cells. Stem Cells *26*, 903–911.

Kuo, C.T., Morrisey, E.E., Anandappa, R., Sigrist, K., Lu, M.M., Parmacek, M.S., Soudais, C., and Leiden, J.M. (1997). GATA4 transcription factor is required for ventral morphogenesis and heart tube formation. Genes Dev. *11*, 1048–1060.

Lin, Y.F., Jing, W., Wu, L., Li, X.Y., Wu, Y., Liu, L., Tang, W., Long, J., Tian, W.D., and Mo, X.M. (2008). Identification of osteo-adipo progenitor cells in fat tissue. Cell Prolif. *41*, 803–812.

Loven, J., Zinin, N., Wahlstrom, T., Muller, I., Brodin, P., Fredlund, E., Ribacke, U., Pivarcsi, A., Pahlman, S., and Henriksson, M. (2010). MYCN-regulated microRNAs repress estrogen receptor-alpha (ESR1) expression and neuronal differentiation in human neuroblastoma. Proc. Natl. Acad. Sci. USA *107*, 1553–1558.

Ma, Z.Q., Spreafico, E., Pollio, G., Santagati, S., Conti, E., Cattaneo, E., and Maggi, A. (1993). Activated estrogen receptor mediates growth arrest and differentiation of a neuroblastoma cell line. Proc. Natl. Acad. Sci. USA *90*, 3740–3744.

Montserrat, N., Nivet, E., Sancho-Martinez, I., Hishida, T., Kumar, S., Miquel, L., Cortina, C., Hishida, Y., Xia, Y., Esteban, C.R., et al. (2013). Reprogramming of human fibroblasts to pluripotency with lineage specifiers. Cell Stem Cell *13*, 341–350.

Niwa, H., Miyazaki, J., and Smith, A.G. (2000). Quantitative expression of Oct-3/4 defines differentiation, dedifferentiation or self-renewal of ES cells. Nat. Genet. *24*, 372–376.

Otto, F., Thornell, A.P., Crompton, T., Denzel, A., Gilmour, K.C., Rosewell, I.R., Stamp, G.W., Beddington, R.S., Mundlos, S., Olsen, B.R., et al. (1997). Cbfa1, a candidate gene for cleidocranial dysplasia syndrome, is essential for osteoblast differentiation and bone development. Cell *89*, 765–771.

Pevny, L., Simon, M.C., Robertson, E., Klein, W.H., Tsai, S.F., D'Agati, V., Orkin, S.H., and Costantini, F. (1991). Erythroid differentiation in chimaeric mice blocked by a targeted mutation in the gene for transcription factor GATA-1. Nature *349*, 257–260.

Rackham, O.J., Firas, J., Fang, H., Oates, M.E., Holmes, M.L., Knaupp, A.S., FANTOM Consortium, Suzuki, H., Nefzger, C.M., Daub, C.O., et al. (2016). A predictive computational framework for direct reprogramming between human cell types. Nat. Genet. *48*, 331–335.

Ralston, A., and Rossant, J. (2005). Genetic regulation of stem cell origins in the mouse embryo. Clin. Genet. *68*, 106–112.

Roeder, I., and Glauche, I. (2006). Towards an understanding of lineage specification in hematopoietic stem cells: a mathematical model for the interaction of transcription factors GATA-1 and PU.1. J. Theor. Biol. *241*, 852–865.

Shi, Y., Desponts, C., Do, J.T., Hahm, H.S., Scholer, H.R., and Ding, S. (2008). Induction of pluripotent stem cells from mouse embryonic fibroblasts by Oct4 and Klf4 with small-molecule compounds. Cell Stem Cell *3*, 568–574.

Shu, J., Wu, C., Wu, Y., Li, Z., Shao, S., Zhao, W., Tang, X., Yang, H., Shen, L., Zuo, X., et al. (2013). Induction of pluripotency in mouse somatic cells with lineage specifiers. Cell *153*, 963–975.

Siebert, H. (2009). Deriving behavior of Boolean bioregulatory networks from subnetwork dynamics. Math. Comput. Sci. *2*, 421–442.

Thomas, R. (1978). Logical analysis of systems comprising feedback loops. J. Theor. Biol. *73*, 631–656.

Voso, M.T., Burn, T.C., Wulf, G., Lim, B., Leone, G., and Tenen, D.G. (1994). Inhibition of hematopoiesis by competitive binding of transcription factor PU.1. Proc. Natl. Acad. Sci. USA *91*, 7932–7936.

Zañudo, J.G.T., and Albert, R. (2013). An effective network reduction approach to find the dynamical repertoire of discrete dynamic networks. Chaos *23*, 025111.

Zañudo, J.G.T., and Albert, R. (2015). Cell fate reprogramming by control of intracellular network dynamics. PLoS Comput. Biol. *11*, e1004193.

Zeineddine, D., Papadimou, E., Chebli, K., Gineste, M., Liu, J., Grey, C., Thurig, S., Behfar, A., Wallace, V.A., Skerjanc, I.S., et al. (2006). Oct-3/4 dose dependently regulates specification of embryonic stem cells toward a cardiac lineage and early heart development. Dev. Cell *11*, 535–546.

Zhang, X., Huang, C.T., Chen, J., Pankratz, M.T., Xi, J., Li, J., Yang, Y., Lavaute, T.M., Li, X.J., Ayala, M., et al. (2010). Pax6 is a human neuroectoderm cell fate determinant. Cell Stem Cell *7*, 90–100.